

Sub-barrier fusion and transfers in the $^{40}\text{Ca} + ^{58,64}\text{Ni}$ systems

D. BOURGIN^{1,2}, S. COURTIN^{1,2,3}, F. HAAS^{1,2}, A. GOASDUFF⁴,
A.M. STEFANINI⁴, G. MONTAGNOLI⁵, D. MONTANARI^{1,2,3}, L. CORRADI⁴,
J. HUIMING⁴, F. SCARLASSARA⁵, E. FIORETTO⁴, C. SIMENEL⁶,
N. ROWLEY⁷, S. SZILNER⁸ and T. MIJATOVIĆ⁸

¹IPHC, Université de Strasbourg, F-67037 Strasbourg, France

² CNRS, UMR7178, F-67037 Strasbourg, France

³ USIAS, Université de Strasbourg, F-67083 Strasbourg, France

⁴ INFN - Laboratori Nazionali di Legnaro, I-35020 Legnaro (Padova), Italy

⁵ Dipartimento di Fisica, Università di Padova, I-35131 Padova, Italy

⁶ School of Physics and Engineering, Australian National University,
Canberra, Australia

⁷ IPN, Université Paris-Sud, F-91406 Orsay, France

⁸ Ruder Bošković Institute, HR-10002 Zagreb, Croatia

Abstract

Fusion cross sections have been measured in the $^{40}\text{Ca} + ^{58}\text{Ni}$ and $^{40}\text{Ca} + ^{64}\text{Ni}$ systems at energies around and below the Coulomb barrier. The ^{40}Ca beam was delivered by the XTU Tandem accelerator of the Laboratori Nazionali di Legnaro and evaporation residues were measured at very forward angles with the LNL electrostatic beam deflector. Coupled-channels calculations were performed which highlight possible strong effects of neutron transfers on the fusion below the barrier in the $^{40}\text{Ca} + ^{64}\text{Ni}$ system. Microscopic time-dependent Hartree-Fock calculations have also been performed for both systems. Preliminary results are shown.

1 Introduction

The fusion process accounts for the major part of the reaction cross section in collisions of heavy ions at above the barrier beam energies. Some of the most striking recent results on the fusion process have nevertheless been obtained for reactions below the Coulomb barrier (CB). At energies around the CB, the process is driven by couplings of the relative motion of the colliding nuclei to their low energy surface vibrations and/or stable deformations. Coupled-channels (CC) calculations taking into account these couplings have proven a very powerful tool to reproduce fusion cross sections at moderate sub-barrier energies. The CC description is discussed in details in a recent review article [1]. Distributions of barriers, extracted from high precision fusion cross section data are also very good tools to test the couplings to collective degrees of freedom of the target and projectile [2]. In the last decade, fusion cross sections have been measured down to the $\sim 1 \mu\text{b}$ level, below effects of the lowest barrier of the distributions of barriers. There, it was found that the measured fusion cross sections decrease sharply, well below predictions of usual CC calculations based on standard Woods-Saxon potentials. This fusion hindrance phenomenon has been shown to depend on the parameters included in the CC calculations and the logarithmic derivative of the energy-weighted cross section is an interesting representation to explore the fusion hindrance phenomenon [3]. The present contribution focusses on fusion measurements at and below the CB for the two $^{40}\text{Ca} + ^{58}\text{Ni}$ and $^{40}\text{Ca} + ^{64}\text{Ni}$ systems.

The starting point of this experimental study is the recent exploration of Ca+Ca systems and also results on Ni+Ni systems. All systems, except $^{40}\text{Ca} + ^{48}\text{Ca}$ have negative Q values for fusion. Fusion excitation functions have been measured for these systems down to very low energies and very low cross sections [4–9].

The ^{58}Ni , ^{60}Ni and ^{64}Ni are vibrational nuclei with well established 1 and 2 phonon states. Most of the Ni+Ni systems have been measured to show hindrance at low energies. The $^{64}\text{Ni} + ^{64}\text{Ni}$ is a textbook case of fusion enhancement and hindrance. For this system, vibrational couplings around the barrier lead to an enhancement of the fusion cross section. These coupling effects get weaker at lower energies and large hindrance is observed. Below the CB, it has been measured that the slope of the fusion excitation function is less steep for the asymmetric $^{58}\text{Ni} + ^{64}\text{Ni}$ system, as regards to the $^{58}\text{Ni} + ^{58}\text{Ni}$ and $^{64}\text{Ni} + ^{64}\text{Ni}$ systems. This was interpreted by the authors by possibly strong positive Q value multiple transfer channels.

In the $^{40,48}\text{Ca}+^{40,48}\text{Ca}$ cases, a fusion hindrance was reported at deep sub-barrier energies for $^{40}\text{Ca} + ^{48}\text{Ca}$. The effect is different for $^{40}\text{Ca} + ^{40}\text{Ca}$ and $^{40}\text{Ca} + ^{48}\text{Ca}$, because of the coupling to the strong 3^- state in the soft ^{40}Ca nucleus with regard to the ^{48}Ca stiff nucleus.

Moreover besides including all couplings to low-lying excited states of the target and projectile in the CC calculations, it has been shown that it is necessary to take into account transfer channel effects to best describe the $^{40}\text{Ca} + ^{48}\text{Ca}$ data. In fact, Q values for the +2n, +3n and +4n transfer channels (from ^{48}Ca towards ^{40}Ca) are positive as well as Q values for the -1p, -2p, -3p and -4p transfer reactions. Other possible particle transfers have negative Q values. In the symmetric $^{40}\text{Ca} + ^{40}\text{Ca}$ and $^{48}\text{Ca} + ^{48}\text{Ca}$ systems, all nucleon transfer channels have negative Q values.

To put it in a nutshell, strong couplings to octupole vibrational states are observed in the fusion of the Ca+Ca systems at CB and below, fusion hindrance is measured at very deep sub-barrier energies in the asymmetric $^{40}\text{Ca} + ^{48}\text{Ca}$ collision as well as effects of neutron transfer channels. The Ni+Ni systems show coupling effects, different from Ca+Ca, but typical of collisions between vibrational nuclei, and presumably the influence of transfer channels in the asymmetric $^{58}\text{Ni} + ^{60}\text{Ni}$ system and even more in the $^{58}\text{Ni} + ^{64}\text{Ni}$ system. Based on the good knowledge of the Ca+Ca and Ni+Ni systems, and effects of couplings under control, we have decided to explore the $^{40}\text{Ca} + ^{58,64}\text{Ni}$ systems at energies around the CB and below to look for eventual transfer effects in the $^{40}\text{Ca} + ^{64}\text{Ni}$ system.

2 Fusion of $^{40}\text{Ca} + ^{58,64}\text{Ni}$

For the $^{40}\text{Ca}+^{64}\text{Ni}$ system, Q values are positive for the +2n to +4n transfer channels. The situation is much less favourable for nucleon transfers for the $^{40}\text{Ca} + ^{58}\text{Ni}$ system: all neutron and proton transfer channels have negative Q values.

A 9 pA intensity $^{40}\text{Ca}^{9+,10+}$ beam was provided by the LNL XTU Tandem with energies ranging from $E_{lab} = 104.75$ MeV to 153.5 MeV in steps of 1.25 MeV below the Coulomb barrier and 2.5 MeV above the Coulomb barrier for both $^{40}\text{Ca} + ^{58}\text{Ni}$ and $^{40}\text{Ca} + ^{64}\text{Ni}$ reactions. The ^{40}Ca beam was impinging on $50 \mu\text{g}\cdot\text{cm}^{-2}$ ^{58}Ni and ^{64}Ni targets deposited on a $20 \mu\text{g}\cdot\text{cm}^{-2}$ ^{12}C backing. The LNL electrostatic beam deflector was used to deflect the incident beam with a rejection factor of 10^7 , and evaporation residues were measured at 2° with a detector set-up composed of 2 micro-channel plate

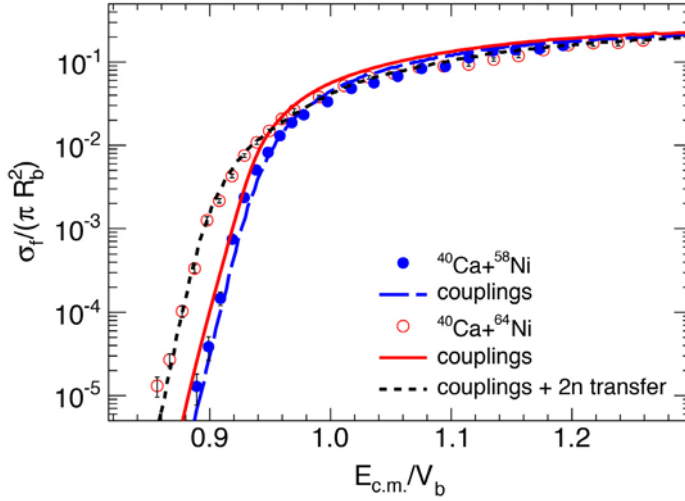


Figure 1: Reduced fusion excitation functions measured in this work for the $^{40}\text{Ca} + ^{58}\text{Ni}$ and $^{40}\text{Ca} + ^{64}\text{Ni}$ systems. The solid and dashed lines are results of CC calculation (see text for details).

detectors, a transverse field ionization chamber and a large silicon detector (600 mm^2). Details on the set-up can be found in [10].

Very accurate fusion cross sections were measured in an energy range from 11 % (resp. 14%) below the CB to 19% (resp. 26%) above the CB for the $^{40}\text{Ca} + ^{58}\text{Ni}$ (resp. $^{40}\text{Ca} + ^{64}\text{Ni}$) system. Fig. 1 shows these fusion excitation functions.

Coupled-channels calculations have been performed for both systems using the CCFULL code [11]. These calculations use a standard O. Akyüz and A. Winther [12, 13] parametrization of the ion-ion potential and relevant couplings to low-lying states of the target and projectile. Parameters of the calculations are given in Table. 1. Interestingly enough, for $^{40}\text{Ca} + ^{58}\text{Ni}$, good description of the cross sections is found including only the octupole 3_1^- state of ^{40}Ca and 2_1^+ state of ^{58}Ni (dashed blue line of Fig. 1). The same type of calculation including couplings to the relevant states, was thus performed for $^{40}\text{Ca} + ^{64}\text{Ni}$. This is shown by the red solid line of Fig. 1. This underestimates the cross sections at sub-barrier energies and it was found that good reproduction of the data is obtained if a 2n transfer channel is included in the CC calculations in some schematical way (black dashed

curve). Neutron transfer channels may thus play an important role in the $^{40}\text{Ca} + ^{64}\text{Ni}$ reaction. More details can be found in [14].

Coupled-channels calculation results are of course sensitive to the number of channels that one take into account. In the next section, we shall present

Table 1: ^{40}Ca , ^{58}Ni and ^{64}Ni spectroscopic data used as parameters of the CC calculations. The transition strengths S and the quadrupole and octupole deformation parameters $\beta_{2,3}$ were determined from the γ -ray energies E_γ of the gs transitions and the mean lifetimes of the states given in Ref. [15].

Nucleus	J^π	E_γ [keV]	S [W.u.]	$\beta_{2,3}$
^{40}Ca	3_1^-	3736	25.95	0.40
^{58}Ni	2_1^+	1454	9.78	0.18
^{64}Ni	2_1^+	1346	7.57	0.16

some preliminary results of alternative calculations based on microscopic methods.

3 Preliminary microscopic TDHF calculations of $^{40}\text{Ca} + ^{58}\text{Ni}$ and $^{40}\text{Ca} + ^{64}\text{Ni}$ reactions

The time-dependant Hartree-Fock (TDHF) method has the advantage that all the couplings are naturally existing at the mean-field level. These can be couplings to surface excitations as well as transfer channels. The method also allows excitations to evolve during the reaction, while the nuclei overlap. Such calculations, using the Sly4 Skyrme energy density fonctionnal, have been performed for both $^{40}\text{Ca} + ^{58}\text{Ni}$ and $^{40}\text{Ca} + ^{64}\text{Ni}$ reactions. Details on the method can be found in [16]. Preliminary results are presented in Fig. 2 which shows the evolution of the nuclear density as a function of time. The corresponding center-of-mass energy is the fusion barrier calculated with the TDHF method, $E_{fus} = 71.70$ MeV and 69.06 MeV for $^{40}\text{Ca} + ^{58}\text{Ni}$ and $^{40}\text{Ca} + ^{64}\text{Ni}$, respectively. The octupole (pear-shaped) deformation of ^{40}Ca during the fusion process is clearly seen on graphs on the 3rd line of the figure (from top, $t = 1.425$ zs). These calculations do not take into account the sub-barrier tunneling. The next step of this study will thus be to use TDHF results such as the frozen potential in CC calculations. This will be the object of a further article.

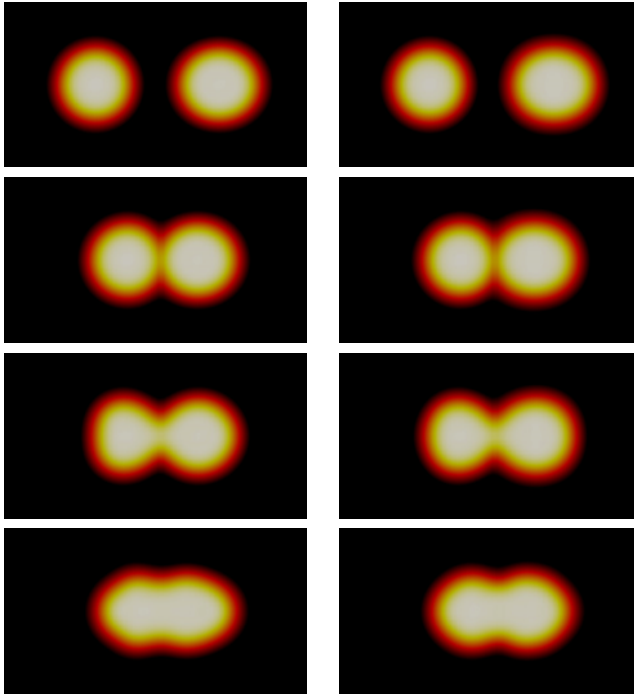


Figure 2: TDHF calculations of the evolution of the nuclear density at the fusion barrier for $^{40}\text{Ca} + ^{58}\text{Ni}$ (graphs at the left) and $^{40}\text{Ca} + ^{64}\text{Ni}$ (graphs at the right). From top to bottom, the time is $t = 0.05$ zs, 0.975 zs, 1.425 zs and 3.15 zs.

4 Conclusions and perspectives

Fusion cross sections have been measured in the $^{40}\text{Ca} + ^{58}\text{Ni}$ and $^{40}\text{Ca} + ^{64}\text{Ni}$ systems at beam energies from 11 % (resp. 14%) below the CB to 19 % (resp. 26%) above the CB for the $^{40}\text{Ca} + ^{58}\text{Ni}$ (resp. $^{40}\text{Ca} + ^{64}\text{Ni}$) system. CC calculations have been performed to describe these fusion cross sections. Hints of strong effects of neutron transfer channels in the $^{40}\text{Ca} + ^{64}\text{Ni}$ system were found. Preliminary TDHF calculations have been performed as well. These have the advantage of taking into account all entrance channel effects during the fusion process.

Following this work, a recent experiment has been performed by our team to measure nucleon transfer cross sections for these systems using the large acceptance magnetic spectrometer PRISMA at LNL. Data is under analysis and should shed light on the importance of transfer in $^{40}\text{Ca} + ^{64}\text{Ni}$ at energies at and below the CB.

5 Acknowledgments

We would like to thank the professional work of the XTU Tandem and target LNL laboratory staff. The research leading to these results has received funding from the European Union Seventh Framework Programme under Grant Agreement No. 262010 ENSAR.

References

- [1] B. B. Back, H. Esbensen, C. L. Jiang, and K. E. Rehm, *Rev. Mod. Phys.* **86** 317 (2014).
- [2] N. Rowley, G.R. Satchler, P.H. Stelson, *Phys. Lett.* **B 254** 25 (1991).
- [3] C.L. Jiang *et al.*, *Phys. Rev. Lett.* **89** 052701 (2002).
- [4] G. Montagnoli *et al.* *Phys. Rev. C* **85** 024607 (2012) and references therein.
- [5] M. Beckerman *et al.*, *Phys. Rev. C* **23** 1581 (1981).
- [6] M. Beckerman *et al.*, *Phys. Rev. Lett.* 1472 (1980).
- [7] D. Ackermann *et al.*, *Nucl. Phys. A* **609** 91 (1996).
- [8] A.M. Stefanini *et al.*, *Phys. Rev. Lett.* **74** 864 (1995).
- [9] C.L. Jiang *et al.*, *Nucl. Phys. A* **834** 615c (2010) and references therein.
- [10] A.M. Stefanini *et al.*, *Phys. Rev. C* **81** 037601 (2010).
- [11] K. Hagino *et al.*, *Comput. Phys. Commun.* **C 123** 143 (1999).
- [12] O. Akyüz, A. Winther, in *Nuclear Structure and Heavy-Ion Physics*, Proc. Int. School of Physics, Enrico Fermi, Varenna, North-Holland, Amsterdam (1981) 492.
- [13] A. Winther, *Nucl. Phys. A* **594** 203 (1995).
- [14] D. Bourgin *et al.*, *Phys. Rev. C* **90** 044610 (2014).
- [15] National Nuclear Data Center, www.nndc.bnl.gov/nudat2.
- [16] C. Simenel, *Eur. Phys. J. A* **48** 152 (2012) and references therein.